Filament spinning of unbleached birch kraft pulps : Effect of pulping intensity on the processability and the fiber properties

Ma, Yibo

2018-01-01

Ma , Y , Stubb , J , Kontro , I , Nieminen , K , Hummel , M & Sixta , H 2018 , ' Filament spinning of unbleached birch kraft pulps : Effect of pulping intensity on the processability and the fiber properties ' , Carbohydrate Polymers , vol. 179 , pp. 145-151 . https://doi.org/10.1016/j.carbpol.2017.09.079

http://hdl.handle.net/10138/307404
https://doi.org/10.1016/j.carbpol.2017.09.079

Filament spinning of unbleached birch kraft pulps: Effect of pulping intensity on the processability and the fiber properties

Yibo Ma[a], Jonas Stubb[a], Inkeri Kontro[b], Kaarlo Nieminen[a], Michael Hummel[a], Herbert Sixta[a].

[a] Y. Ma, Dr. M. Hummel, Prof. H. Sixta
Department of Forest Products Technology
School of Chemical Technology
Aalto University
P.O. Box 16300, 00076 Aalto (Finland)
E-mail: herbert.sixta@aalto.fi

[b] I. Kontro.
Division of Material physics, Department of Physics
Helsinki University
P.O. Box 64, FI-00014, (Finland)

Highlights

- Man-made fibres were spun from low refined kraft pulps.
- E-beam as dry, non-chemical treatment was used for DP adjustment of lignocellulose.
- The effect of the chemical compositions on the spinnability is only minor.
- The spinnability is mainly dependent on the molecular integrity of lignocellulose matrix.

ABSTRACT Man-made lignocellulosic fibres were successfully prepared from unbleached birch kraft pulps by using the IONCELL-F technology. Pulps with different lignin content were produced by tailored kraft pulping with varying intensity. The degree of polymerization of the pulps was adjusted by acid-catalyzed hydrolysis and electron beam treatment. All substrates were completely soluble in 1,5-diazabicyclo[4.3.0]non-5-enium acetate ([DBNH]OAc) and the respective solutions were spinnable to yield fibres with good to excellent mechanical properties despite the use of only mildly refined wood pulp. The tensile properties decreased gradually as the lignin concentration in the fibres increased. Changes in the chemical composition also affected the structure and morphology of the fibres. Both the molecular orientation and the crystallinity decreased while the presence of lignin enhanced the water accessibility. The effects of the crystallite size and lignin content on monolayer water adsorption are discussed.

Keywords*: Lignocellulose, fibres, refining, spinning, ionic liquid.*

1. INTRODUCTION

The global demand of textile fibres is gradually increasing in response to the global megatrends such as population and prosperity growth in combination with sustainability thinking and the limited increase in the production capacities of cotton. Thus, more man-made cellulosic fibres (MMCFs) are potentially needed to fill the 'fibre demand gap' in the future (Hämmerle, 2011). Currently, the major markets of MMCFs are dominated by viscose and Lyocell fibres. However, the viscose fibre process is connected to environmental and safety concerns due to the utilization of CS_2 for the intermediate derivatization of cellulose into cellulose xanthate (Hermanutz, Meister, & Uerdingen, 2006). In addition to the mentioned drawbacks of this process, this technology demands dissolving pulp as feedstock. In the viscose process, the presence of lignin and hemicellulose will deteriorate the xanthation of the pulp and process filterability drastically. This results in poor spinnability, if processable at all (Hans Peter Fink et al., 2004; Gübitz, Stebbing, Johansson, & Saddler, 1998). The Lyocell process is an environmentally friendly process in which both the cellulose solvent and spent water are fully recovered and circulated. This process allows for the direct dissolution of cellulose to yield a spin dope that is processed through dry-jet wet spinning. The spun fibres are clearly stronger than regular viscose fibres. Despite the advantages of the Lyocell process, the process operates at a relatively high temperature and requires the addition of stabilizers to prevent dangerous runaway reactions during the dope preparation and spinning (H P Fink, Weigel, Purz, & Ganster, 2001). From the feedstock point of view, the NMMO-based Lyocell process can already utilize dissolving pulp, paper grade pulp (with high hemicellulose content) and even unbleached chemical pulp for fibre production (Rosenau, Potthast, Sixta, & Kosma, 2001). However, NMMO, as an oxidant, might react with the lignin present in the raw material to unexpected degradation reaction, especially at high temperatures between 110 and 130 ºC as typically used in the NMMO process. Furthermore, the dissolution of

the raw material in NMMO could be more difficult, thus affecting the quality of the dope which may lead to spinnability problems (Hans Peter Fink et al., 2004).

The IONCELL-F process is a recently developed process in which the ionic liquid 1,5-diazabicyclo [4.3.0]non-5-enium acetate ([DBNH][OAc]) is utilized as a solvent for cellulosic material and the resulting dope is processed in a dry jet-wet spinning process to form filaments with high mechanical properties (Hummel et al., 2015; A Michud et al., 2014; Parviainen et al., 2013; Sixta et al., 2015). The IONCELL-F process, a Lyocell-type fibre process, is considered to be a green fibre spinning technology. It has been shown that it is largely insensitive to the composition of lignocellulosic material and tolerates varying amounts of non-cellulosic components such as lignin and hemicelluloses (Y Ma et al., 2016; Yibo Ma et al., 2015a). Thus, it is not necessary to source highly refined dissolving pulp for this spinning process.

In previous studies (Le, Ma, Borrega, & Sixta, 2016; Y Ma et al., 2016), we have demonstrated the possibility to spin unbleached organosolv pulps, waste fine paper and pre-treated waste cardboard in IL solution and the spun fibres showed good to excellent properties. However, untreated waste cardboard (made from mainly low-refined semi-chemical pulp), which contains a large lignin content, cannot be dissolved in the IL completely. The spinning dope resulting from the untreated waste cardboard behaves likes a gel, which can only be spun with low draw ratio and the fibre properties were unacceptably low for commercial and technical applications. Jiang et al.(Jiang, Sun, Hao, & Chen, 2011) and Sun et al.(Sun et al., 2011) have also reported the possibility of spinning fibres from lignocellulosics using IL as a solvent. However, due to the presence of lignin and hemicellulose, the spun fibres showed rather low mechanical properties, not suitable for commercial use. To confirm the negative effect of native lignin on the solubility and spinnability, polymer blends of cellulose and lignin with different ratio were subjected to

dissolution and fibre spinning (Yibo Ma et al., 2015a). Different to the native lignocellulosic material, the polymer blends with up to 50% lignin can be readily dissolved in IL and the fibres produced from the IL – polymer dope show good mechanical properties. Presumably, lignin molecules embedded in the cell wall architecture are associated with polysaccharides, mainly hemicellulose, forming lignin-carbohydrate complexes (LCCs), which hamper the complete dissolution of the native lignocellulosics in IL and leads to a gel-like solution, respectively (Hauru et al., 2013; Sun et al., 2009).

The main objectives of the study at hand are to investigate the spinnability of unbleached, hemicellulose-rich kraft pulps from birch wood. The primary goal is to identify the critical content of native lignin at which the pulp cannot be dissolved efficiently in an IL solvent and thus, results in poor spinnability. The findings from this research work provide valuable information on the necessary minimum refining degree for the dry-jet wet spinning of lignocellulosic material.

2. Experimental Section

2.1 Kraft cooking

Birchwood (*Betula pendula*) chips were provided by Metla, Finland. The dissolving grade birch prehydrolyzed kraft (PHK) pulp (Enocell Pulp) was kindly supplied by Stora Enso, Finland. The birchwood chips were screened according to standard SCAN-N 2:88 prior to kraft cooking. The cooking was executed in 2 L autoclaves attached in a rotary air bath digester. The cooking conditions are list in Table S1. Pulp samples were taken at H-factor (Sixta, 2006) 25, 50, 200, 500, 800, 1000 and 1200. These samples will be referred to as H25, H50 etc. After kraft cooking, the black liquor was removed and the pulps were washed. The kraft pulps H1200, H1000, H800 and H500 were subjected to screening with a Mänttä flat screen using a screen plate with a slot width

of 0.35 mm. The screening rejects were collected from the screen plate and dried in an oven at 105 ºC for the determination of the rejects content. Due to the low degree of refining, the pulps H200, H50 and H25 could not be defibrillated manually. Thus, a disc refiner was utilized for pulp defibration. These samples were not screened due to the large amount of oversize fibers.

2.2 Degree of polymerization (DP) adjustments

The DP of the refined material was adjusted using two methods: acid-catalyzed hydrolysis and electron beam (E-beam) irradiation treatment. The acid-catalyzed hydrolysis was done in the same autoclave as was used for the kraft cooking. 5 samples, derived from H1200, H1000, H800, H500 and H200, were selected for the acid-catalyzed hydrolysis. The hydrolysis was accomplished for 2 hours at 130 ºC with an acid concentration of 6 g/l. The samples were then washed and air-dried for further use.

Birch PHK, birch H50 and birch H25 pulps were irradiated at LEONI Studer AG, Switzerland, with a 10 MeV Rhodotron TT300 accelerator built by IBA for DP adjustment. Prior to E-beam treatment, pulp sheets (thickness is 0.15 mm for each sheet) were prepared using a laboratory sheet former. For establishing a dosage-DP relationship, the E-beam dosages were varied from 5 to 30 kGy for the different pulps. The large batch treatment for H25 and H50 pulps was performed at an E-beam dosage of 20 kGy.

2.3 Pulp dissolution

[DBNH][OAc] was first melted at 70 ºC, then blended with the air-dried pulp (ground with a Willey mill with 1 mm mesh sieves), stirred for 1.5 h at 80 ºC with 10 rpm at reduced pressure (50–200 mbar) using a vertical kneader system. The polymer concentration of the dope was adjusted to 13 or 15 wt% according to the intrinsic viscosity of the pulps. The solutions were filtered through a hydraulic press filter device (metal filter mesh with 5 µm absolute fineness, Gebr.

Kufferath AG, Germany) at 2 MPa and 80 ºC to remove undissolved substrate, which would lead to unstable spinning. The prepared dope was finally shaped into the dimensions of the spinning cylinder and solidified upon cooling overnight to ensure filling without inclusion of air bubbles.

2.3 Spinning trials

Multi-filaments were spun with a customized laboratory piston spinning system (Fourné Polymertechnik, Germany). The solidified spinning dope was heated to 70 ºC in the spinning cylinder to form a highly viscous, air-bubble-free spinning dope. The molten solution was then extruded through a 36-hole spinneret with a capillary diameter of 100 µm and a length to diameter ratio (L/D) of 0.2. After the generated filaments had passed an air gap of 10 mm, they were coagulated in a water bath (10 to 15 ºC) in which they were guided by Teflon rollers to the godet couple. The extrusion velocity (V_e) was set to 1.6 ml/min (5.66 m/min), while the take-up velocity (V_t) of the godet was varied from 5 to 85 m/min to reach the maximum draw ratio (DR= V_t/V_e) at which stable spinning was ensured. The fibres were washed off-line in hot water (60 °C) and air-dried. The analytical methods of the raw materials, spinning dopes and spun fires including were carried out according to Yibo Ma et al. (2015b) and were presented in ESI section 1.

3. Results and Discussion

3.1 Pulp properties

To obtain pulps with different lignin content, seven birch wood kraft pulps (from H-factor 1200 to 25) were produced by means of a conventional kraft cooking method. As expected (and shown in Table S1), the pulp yield before screening decreases as the H-factor increases. Pulp screening was not possible for low refined pulps H25, H50, H200 due to incomplete defibration. Therefore, the yield after screening could not be determined. The intrinsic viscosity of the different pulp samples was almost at the same level. A significant reduction in viscosity was observed for H25

and 50. This is likely an artifact resulting from the low refining which prevents the dissolution of high molecular weight fractions of pulp in CED.

Birch wood kraft pulps from H200 to H1200 were subjected to acid catalyzed hydrolysis in order to reduce the intrinsic viscosity (optimal range 420 to 450 ml/g), which has been identified earlier as optimum viscosity level to yield spinnable solutions. Table 1 lists the intrinsic viscosity (η_0) of the pulps before and after the hydrolysis. The viscosity of the pulps was efficiently reduced by acid catalyzed hydrolysis, albeit to a slightly lower level than initially aimed at. Concomitantly, low molecular weight hemicelluloses were also degraded to such an extent that they became soluble in the reaction liquor (Mosier et al., 2005). These phenomena were reflected by the MMD as shown in Figure S1. Untreated pulps revealed a bimodal MMD (representing low-molecular weight hemicellulose and high-molecular weight cellulose). However, as expected, after acidic hydrolysis and further conversion to regenerated fibers (through dissolution in IL and regeneration during the spinning process) the low molar mass peaks almost disappeared, leaving a cellulose peak with a subtle shoulder at relatively low molar mass.

Table 1. Intrinsic viscosity and chemical compositions of the original and DP adjusted kraft pulps and their spun fibres.

	Original kraft pulp				DP adjusted pulps				Fibres		
Samples	Cellulose	Hemicellulose	Lignin	η_0 ml/g	Cellulose	Hemicellulose	Lignin	η_0 ml/g	Cellulose	Hemicellulose	Lignin
H25	53.7	22.4	23.9	-	-	-	-	-	55.8	20.2	24.0
H50	56.4	21.8	21.8	-	-	-	-	-	57.9	21.7	20.4
H200	63.6	21.9	14.5	1795	75.1	9.8	15.1	361	75.2	6.1	18.7
H500	68.9	22.5	8.6	1591	83.6	7.9	8.5	390	85.9	5.2	8.9
H800	71.2	23.0	5.8	1626	84.6	10.4	5.0	367	88.5	6.9	4.6
H1000	72.0	22.6	5.4	1656	85.0	10.2	4.8	403	88.1	8.0	3.9
H1200	72.7	22.2	5.1	1599	85.9	9.8	4.3	351	87.8	7.2	5.0

The chemical composition of the initial kraft pulps, the DP adjusted pulps, and the spun fibres are summarized in Table 1. The hemicellulose content of acid hydrolyzed pulps is notably lower than in the kraft pulps. Furthermore, there is a slight decrease in the lignin content. The reduction in the hemicellulose and lignin contents result in a rise in the relative cellulose concentration of the pulp, which facilitates the subsequent fiber spinning.

Birchwood kraft pulps H25, H50 were subjected to electron beam irradiation treatment. Electron beam irradiation is an environmental friendly pre-treatment technology for lignocellulosic biomass, that reduces the molecular weight and crystallinity by breaking chemical bonds in cellulose, hemicellulose and lignin (Khan, Labrie, & McKeown, 1986; Kristiani, Effendi, Styarini, Aulia, & Sudiyani, 2016; Lee et al., 2014). Prior to the main trials, several E-beam dosages had been screened in order to find the optimal radiation dosage for the DP adjustment. Pre-hydrolyzed birch kraft pulp and pine kraft paper pulp were selected as model pulps that were treated together with H25 and H50 by E-beam dosages from 5 to 30 kGy. E-beam treatment – especially at such low irradiation intensity – was expected to not alter the chemical compositions of the pulps (Imamura, Murakami, & Ueno, 1972; Kassim et al., 2016; Kristiani et al., 2016). Figure 1 presents the intrinsic viscosity of the original and the E-beam treated kraft pulps as a function of the irradiation dosages. A pronounced decrease in intrinsic viscosity (DP) was visible already at 10 kGy. The viscosity then tended to decrease gradually upon progressive increase of the E-beam dosage. This finding confirmed that E-beam irradiation is a suitable method to reduce the polymer-DP through chain scission (Imamura et al., 1972).

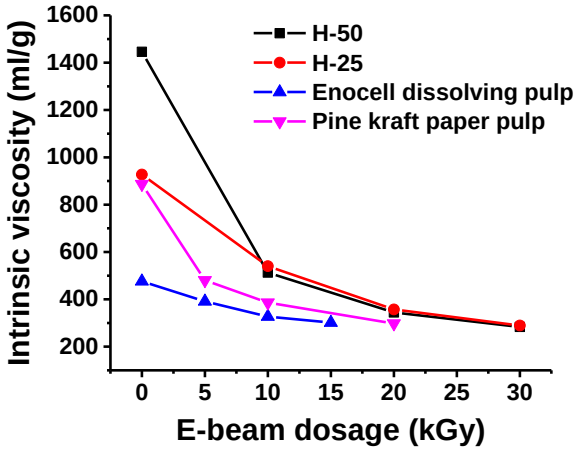

Figure 1. The intrinsic viscosity of E-beam treated H25 and H50 samples and a reference birch PHK pulp.

To assess the effects of E-beam treatment on the carbohydrates in more detail, the molecular weight distribution of the E-beam treated pulps was analyzed (Figure S2). Typically, a bimodal molecular weight distribution was obtained for all the measured samples. The results of GPC measurements clearly demonstrated that the high molecular weight domains shifted to lower molar mass, while the molecular weight of the short-chain fraction remained unchanged. This is in agreement with the intrinsic viscosity measurement where the intrinsic viscosity decreases as E-beam dosage increases.

3.2 Dissolution and dope properties

Spinning dopes were prepared in [DBNH]OAc with the acid hydrolyzed kraft pulp from H1200 to H200 and E-beam treated (20 kGy) kraft pulps H25 and H50. The rheological properties of the dopes were determined via oscillatory shear measurements yielding the complex viscosity and dynamic moduli as a function of the angular frequency. The crossover point of the dynamic moduli

and the zero shear viscosity were calculated using the Cross model and assuming the validity of the Cox-Merz rule (Hummel et al., 2015). In previous studies (Sixta et al., 2015), it was found that stable spinning is possible if the zero shear viscosity of the spin dope is around 30 000 Pa.s and the crossover modulus ranges between 3000 and 5000 Pa at a crossover frequency of around 1 s^{-1}. Several subsequent studies (Asaadi et al., 2016; Yibo Ma et al., 2015a; A Michud et al., 2014; Anne Michud, Tanttu, et al., 2016) have confirmed these requirements for successful fibre spinning. However, a successful fibre spinning was observed when attempting to spin a spinning dope from an unbleached pulp, of which the rheology was outside the optimal spinning window (Y Ma et al., 2016).

Since the molar mass distribution and the DP of the raw material are crucial for the viscoelastic properties of the spinning dope, the selection of the polymer concentration (or spinning temperatures) has to be adjusted in order to meet the above-mentioned dope properties (Anne Michud, Hummel, & Sixta, 2015, 2016). Because of the low intrinsic viscosity of the resulting acid hydrolyzed kraft pulps, H1200 and H1000, a 15 wt% concentration of these pulps in [DBNH]OAc was prepared to adjust the required viscoelastic properties and thus to ensure their spinnability. Contrary to our expectation, these two dopes exhibited a high complex viscosity without a Newtonian plateau within the measured angular frequency range (gel-like power-law dependency). To reduce the dope viscosity, spinning dopes from H800, H500 and H200 were prepared with a polymer concentration of 13 wt%. However, only two of them, the H800 and H500-derived dopes, revealed the expected complex viscosity typical for spinnable solutions (Figure 2A). The zero shear viscosity of the spinning dopes from H200 to H1200 is listed in Table S2. At a low H-factor of H200, the respective dope showed a strong gel-character even at 13 wt% polymer concentration and despite a low pulp intrinsic pulp viscosity. This was attributed to a

lignin with a relatively high content of 15%, which is presumably bond to hemicellulose and/or cellulose to form lignin-carbohydrate complexes (LCC). Thus, it can be hypothesized that residual lignin embedded in the cell wall architecture acts as a crosslinker between the carbohydrate polymer chains, which tend to form extended aggregates in solution exhibiting a gel behavior of the resulting dope.

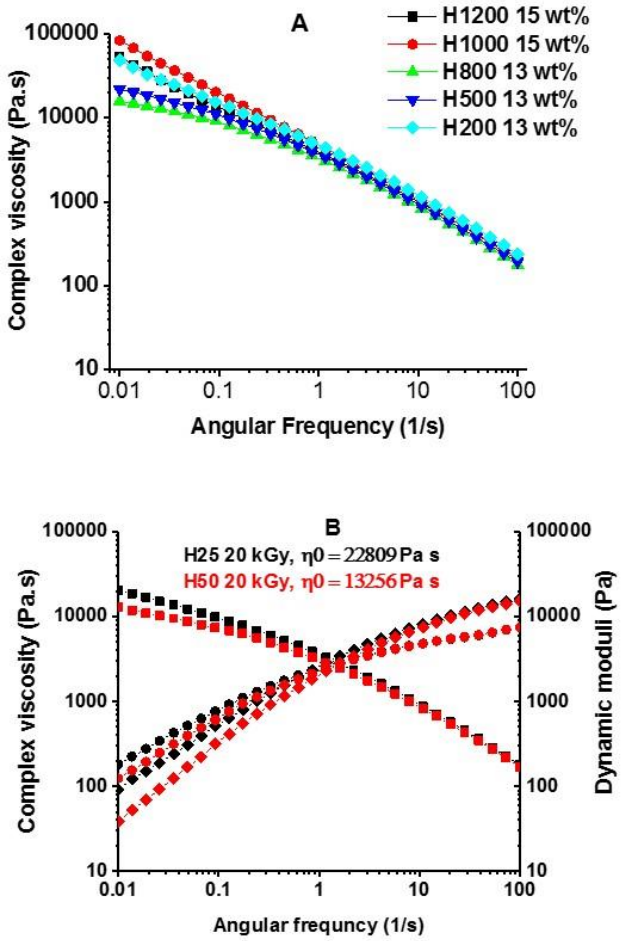

Figure 2. A) Complex viscosity of the spinning dopes from H200 to H1200 at the spinning temperatures. B) Complex viscosity and dynamic moduli of E-beam treated kraft pulps H25 and H50 at 70 ºC. ■: Complex viscosity. ♦: Storage modulus. ●: Loss modulus.

The E-beam treated birch kraft pulps (20 kGy, H25 and H50) were dissolved in [DBNH]OAc at a polymer concentration of 13 wt%. Figure 2B illustrates the viscoelastic properties of the E-beam treated pulps. Unlike a solution from H200, these two dopes did not show any gel behavior regardless of the high lignin content. This could be explained by the efficient cleavage of the cellulose and lignin chains as well as the LCC bonds by the electron beam irradiation (Bak, 2014). Direct comparison of the viscoelastic properties of the dopes prepared from H25 and H50, revealed a more pronounced solution state for the H50. At high angular frequency complex viscosity and dynamic moduli of the two dopes were almost perfectly superimposed. At low angular frequency the complex viscosity of the H50 dope started to enter the Newtonian plateau whereas the complex viscosity of the H25 dope continues to raise. As a result, the zero shear viscosity of H25 dope was higher than that from the H50 dope.

3.3 Dope spinnability and tensile properties of the spun fibres

The spinning performance depends on several factors of which most are connected to the dope rheology. The polymer solution must exhibit the right fluidity to be extruded through the spinneret orifices. Further, a dry-jet wet spinning process demands the stretch of the filaments in the air gap. Hence, the filaments must have a certain visco-elasticity to withstand the draw without rupture. We have thus defined spinnability in terms of accessible draw ratios: DR<2 non-spinnable, 2–8 poor, 8–14 good, >14 excellent spinnability. All dopes showed good to excellent spinnability. In the case of acid hydrolyzed kraft pulps, only H1200 showed a relative low spinnability (reflected by the low draw ratio of 8.8). Considering the high cellulose content in H1200, a better spinning performance was expected. Possibly, the high dope viscosity and the relatively high spinning temperature may have limited the spinnability. The solution prepared from the H800 pulp showed the highest spinnability with a maximum draw ratio of 17.7. Surprisingly, the dopes from H200,

H50 and H25, which contained large amounts of lignin and hemicellulose, were still spinnable and showed good spinnability (15.9 for H200 and 9.7 for both H25 and 50). Table 2 summarizes the mechanical properties of the spun fibres. The fibre tenacity is closely linked with the cellulose microfibril orientation in the fibre (H P Fink et al., 2001; Kong & Eichhorn, 2005). A high draw ratio results in fibres with more pronounced lateral orientation of the polymer chain, therefore, yields fibres with improved tenacity. Due to the low spinnability, the fibre spun form H1200 dope had the lowest conditioned (32.9 cN/tex) and wet tenacity (19.9 cN/tex) among the fibres from acid hydrolyzed kraft pulps, while the H800 fibre showed the highest conditioned tenacity of 40.2 cN/tex and wet tenacity of 29.3 cN/tex due to the excellent spinnability of the dope. The lignin and hemicellulose content do not only affect the spinnability, but also influence the mechanical properties of the spun fibres through their relatively low DP and their inability to orient themselves along the molecular axis. Because the lignin contents in H200, H50 and H25 pulps are significantly higher as compared to the other pulps, the mechanical properties of the resulting fibres were notably reduced. Especially, the fibres spun from the H50 and H25 pulps reveal a conditioned tenacity of only 24.4 and 23.0 cN/tex, which may be explained by a very low cellulose content of 56% and 58%, respectively (Table 2).

Table 2. Tensile properties of the spun fibres from H1200 to H200 dopes.

Samples	Draw ratio	Titer (dtex)	Dry elongation (%)	Dry tenacity (cN/tex)	Wet elongation (%)	Wet tenacity (cN/tex)
H25	9.7	2.02	8.1	23.0	7.7	11.1
H50	9.7	2.14	7.4	24.4	7.0	13.7
H200	15.9	1.71	7.6	32.1	8.8	20.1
H500	12.4	1.78	9.0	38.1	9.2	26.1
H800	17.7	1.43	7.7	40.2	9.7	29.3
H1000	15.9	1.58	8.0	37.3	8.6	24.9
H1200	8.8	2.74	9.2	32.9	9.4	19.9
Lyocell	-	1.3	9.5	34.3	-	-

3.4 Structural properties of fibres

As stated above, the tensile properties of the fibre are directly connected to the cellulose orientation. The total orientation of cellulose molecules in a fiber matrix can be assessed by means of birefringence measurement. In agreement with the previous studies (Asaadi et al., 2016; Yibo Ma et al., 2015a), the degree of orientation of the fibers increased significantly at low draw ratio and tends to level-off when exceeding a draw ratio of 5. A slight drop in the orientation might occur at higher draw ratio due to relaxation of the cellulose molecules, which is caused by the slippage of cellulose chains and the breakage of the intermolecular hydrogen bonds among the cellulose molecules (Asaadi et al., 2016; Kong & Eichhorn, 2005). Figure 3 shows that the total degree of orientation was affected by both the lignin concentration and the spinnability, characterized by the draw ratio during spinning. Surprisingly, H1200 fibres that could be produced only at relatively low draw ratio showed an overall lower orientation than pulps with a similar composition. In the case of H200, H50 and H25 fibres, having a significantly higher lignin content, the total orientation was notably reduced. The presence of lignin disturbs the highly ordered structure formed by cellulose chains and, thus, reduces the total orientation of the fiber (Kong & Eichhorn, 2005). The development of the degree of orientation is consistent with the tensile properties of the fibres. A reduction of total orientation caused a decrease of the fibre tenacity.

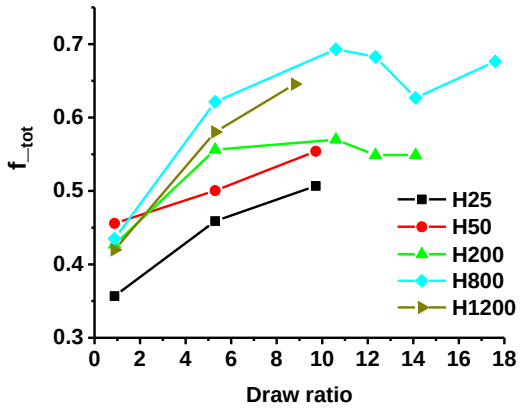

Figure 3. Degree of total orientation f_{tot} of the fibres at selected draw ratios.

The crystallinity and the crystallite size of fibres listed in Table 3 were assessed by XRD measurement. The XRD spectra of selected samples are shown in Figure S3. The crystallinity of the fibres increases upon progressive cooking intensity of pulp production, with the fibre spun from the H1200 pulp having the largest crystallinity of 50%. The increase in the lignin content of the fibres spun from kraft pulps prepared with gradually decreased cooking intensity (from H-factor 200 to H-factor 25) results in a crystallinity drop to 43% and 40% in relation to the total sample, respectively. The crystallite dimensions were assessed in 110, 1-10 and 020 direction and extrapolated by using the Scherrer equation (Leppänen et al., 2011). The crystallite width measured in 110 direction (perpendicular to the cellulose crystal plane) follows the trend of the degree of crystallinity. By contrast, there is no distinct difference observed in the crystalline width in 1-10 direction. However, it has to be noted that the fit quality of the 110 and 1-10 crystallite width suffered from the overlap of the respective peaks. Furthermore, it has been shown that the signals from 110 and 1-10 may include crystal aggregations or less ordered cellulose chains on the surface which result in erroneous values for the crystallite width (Cheng et al., 2011; Maurer, Sax, & Ribitsch, 2013). In general, the crystallite width estimated in 020 direction (sharp peak from 22 to 25º with high intensity in the XRD diffractograms) is more reliable. However, no distinct

correlation between the 020 crystallite width and the lignin content (i.e. pretreatment intensity) was observed.

Table 3. Crystallinity and crystallite width analyzed by XRD from the H1200, H800, H200, H50 and H25 fibres at the highest draw ratio.

Samples	Draw ratio	Crystallinity index (%)	Crystallite width (nm)		
			110	$1\bar{1}0$	020
H25	9.7	40±3	2.6±0.15	3.2±0.3	5.7±0.3
H50	9.7	40±3	2.9±0.15	3.2±0.3	6.0±0.3
H200	15.9	43±3	3.4±0.15	2.9±0.3	5.6±0.3
H800	17.7	48±3	3.8±0.15	2.9±0.3	5.8±0.3
H1200	8.8	50±3	3.8±0.15	3.1±0.3	5.5±0.3

Scanning electron microscopy images of the fibres (surfaces and cross sections) were recorded in order to examine their structural alterations along their compositional changes (Figure 4). Indeed, SEM images reveal a significant effect of the pretreatment intensity on the structure of the fibre. When the fibres contained a higher amount of lignin (H25 and H200), the microfibrils became less orientated and voids were clearly visible in the SEM images of the cross section. Consequently, the fibres become more ductile which leads to a loose structure. When the cellulose content increased (H800 and H1200), the orientation of the cellulose microfibrils became more pronounced and the fibre surfaces appeared smooth.

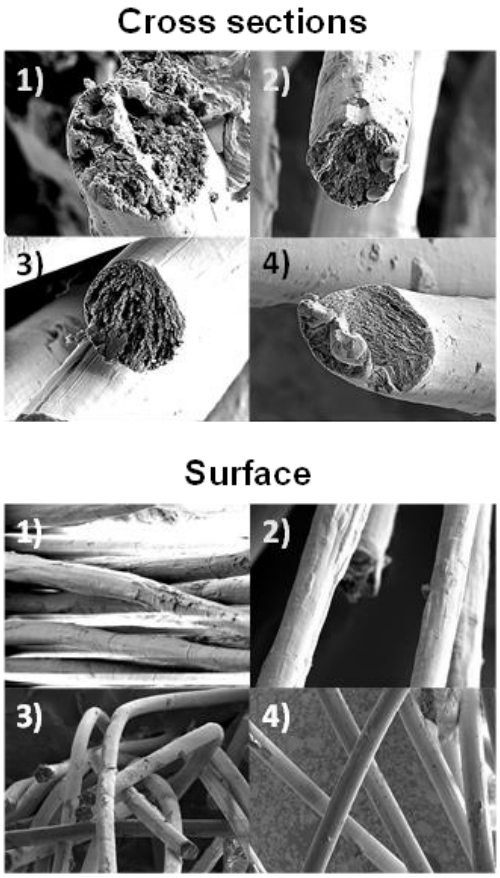

Figure 4. SEM images of fibres cross sections (top) and surface (bottom); 1) H25, 2) H200, 3) H800 and 4) H1200.

Dynamic vapour sorption (DVS) studies were conducted to gain further insight into the relationship between the structural and chemical characteristics of the fibers. Water sorption behavior of regenerated cellulosic fibres depends on several factors, e.g. morphology, crystallinity, degree of orientation and the chemical compositions (Bingham, 1964; Kreze & Malej, 2003; Okubayashi, Griesser, & Bechtold, 2004, 2005b, 2005a; Siroka, Noisternig, Griesser, & Bechtold, 2008; Stana-Kleinschek, Ribitsch, Kreže, Sfiligoj-Smole, & Peršin, 2003). It has been shown that Lyocell type fibres absorb a little bit less moisture compared to viscose fibres due to their higher degree of orientation (which is closely related to crystallinity) and more compact structure.

However, when lignin as a hydrophobic component is present in the fibres it may hamper the moisture absorption as was observed earlier (Yibo Ma et al., 2015a). Figure 5 illustrates the equilibrium moisture sorption and desorption isotherms of tested fibres (a) and shows their hysteresis (b).

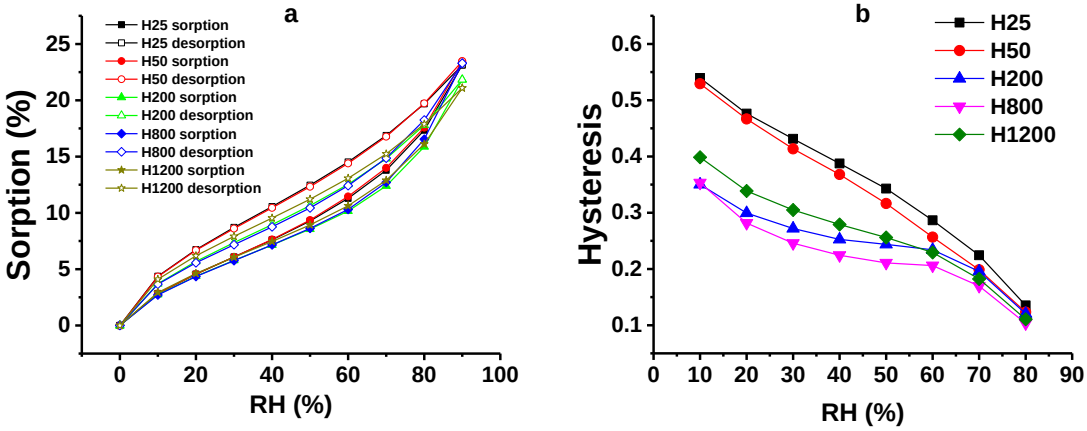

Figure 5. Equilibrium moisture isotherms of spun fibres (a) and the hystereses of the sorption and desorption isotherms from H25, H50, H200, H800 and H1200 fibres (b).

Comparing with the previous studies on the DVS of man-made cellulose fibres (Okubayashi et al., 2004, 2005a, 2005b), a similar moisture sorption and desorption development was found with the fibres spun from kraft pulp/ionic liquid dopes, which is typical for cellulosic materials. Contrary to our expectation, lignin did not act as a moisture repellent in these fibres. However, it contributed more to the loss of the fibre orientation together with hemicellulose. Thus, a clear effect of the degree of orientation on the wetting of the fibres was noted. Moreover, the role of the cellulose crystallite size (derived from the 020 reflection) on the monolayer (ML) hydration has been investigated based on the theory proposed by Driemeier (Driemeier & Bragatto, 2013) using the Hailwood-Horrobin (HH) model (Hailwood & Horrobin, 1946; Skaar, 1988) with lignin-free

cellulose I samples. However, no clear relationship between ML water sorption and reciprocal crystallite width could be identified, because of the presence of lignin and different crystal structure in our spun fibres (see ESI section 4, Table S2). Lignin, hemicellulose and the degree of orientation seem to be more dominant factors.

To further exhibit the influence of the chemical composition/total orientation of the spun fibres on the water sorption/desorption (presented as ML water sorption, desorption and their hysteresis), multiple regression analysis was carried out with lignin content, hemicellulose content and total orientation as predictor variables. The multiple regression equations are listed in the ESI, section 4. In this work, the three predictor variables are collinear, from which it is possible to express e.g. the total orientation as a linear combination of the other two variables. Thus, there is no need to estimate the responses of the ML water sorption/desorption for any arbitrary combination of the predictor variables. In this scenario, the total orientation could be used as third predictor and restricted to an interval centered around the value obtained by linearly fitting the total orientation to the other predictors. The responses of ML water sorption/desorption are visualized (shown as contour plots in Figure S3-5), in which lignin and hemicellulose are predictors at different levels of aberration of the total variables. The interpretation of the visualization almost proved that the wetting behavior is largely dependent on the chemical composition and the total orientation of the fibre. According to Figure S3, the ML sorption slightly decreases with the hemicellulose content and increases with the lignin content as well as with the total orientation. Figure S4 allows for a similar interpretation on ML desorption, but with the exception that increasing hemicellulose content causes a slight raise on the ML water desorption. Eventually, Figure S5 reveals that increasing the hemicellulose and lignin content simultaneously increases the hysteresis, whereas the increasing total orientation once again has a decreasing effect. However, it has to be stressed

that the five data points are not enough for a compelling regression analysis in three variables. Hence, the regression is rather a means of comprehensively visualizing the observed responses at different values of the predictor variables.

4. CONCLUSION

1,5-diazabicyclo[4.3.0]non-5-enium acetate is a promising biopolymer solvent for the production of high quality fibres, not only from costly dissolving pulps but also from low-refined unbleached pulps. In this study, our objective to find a limit in the lignin content was not achieved; even at the highest lignin content the pulp was still spinnable. The fibres showed good to excellent mechanical properties. The spinnability was primarily dependent on the macromolecular integrity of the carbohydrate matrix but not as much on its composition. Contrary to our previous study, the lignin present in the fibre did not render the fibre hydrophobic. However, it reduced the total orientation of the fibre, which leads to a more pronounced wetting of the fibre.

Most importantly, E-beam irradiation was identified as an environmentally friendly alternative for DP adjustment and production of fibres from unbleached birch kraft pulp with varying amount of lignin and hemicellulose. Contrary to the DP adjustment with an acid treatment, E-beam irradiation does not yield any material losses. This increases the overall process economy and environmental sustainability of the Ioncell-F technology. For further work, a milder pre-treatment in combination with E-beam irradiation (which cleaves the LCC bonds) is still necessary to investigate the spinning limitation.

Acknowledgements

This study is part of the ''Design Driven Value Chains in the World of Cellulose'' project funded by the Finnish Funding Agency for Innovation (TEKES). The authors would like to thank Rita Hataka for performing carbohydrate and molar mass distribution analyses.

References

Asaadi, S., Hummel, M., Hellsten, S., Härkäsalmi, T., Ma, Y., Michud, A., & Sixta, H. (2016). Renewable High-Performance Fibers from the Chemical Recycling of Cotton Waste Utilizing an Ionic Liquid. *ChemSusChem*, *9*(22), 3250–3258. https://doi.org/10.1002/cssc.201600680

Bak, J. S. (2014). Electron beam irradiation enhances the digestibility and fermentation yield of water-soaked lignocellulosic biomass. *Biotechnology Reports*, *4*, 30–33. https://doi.org///dx.doi.org/10.1016/j.btre.2014.07.006

Bingham, B. E. M. (1964). A study of the fine structure of regenerated cellulose fibers. *Die Makromolekulare Chemie*, *77*(1), 139–152. https://doi.org/10.1002/macp.1964.020770113

Cheng, G., Varanasi, P., Li, C., Liu, H., Melnichenko, Y. B., Simmons, B. A., … Singh, S. (2011). Transition of Cellulose Crystalline Structure and Surface Morphology of Biomass as a Function of Ionic Liquid Pretreatment and Its Relation to Enzymatic Hydrolysis. *Biomacromolecules*, *12*(4), 933–941. https://doi.org/10.1021/bm101240z

Driemeier, C., & Bragatto, J. (2013). Crystallite Width Determines Monolayer Hydration across a Wide Spectrum of Celluloses Isolated from Plants. *The Journal of Physical Chemistry B*, *117*(1), 415–421. https://doi.org/10.1021/jp309948h

Fink, H. P., Weigel, P., Ganster, J., Rihm, R., Puls, J., Sixta, H., & Parajo, J. C. (2004). Evaluation

439 of new organosolv dissolving pulps. Part II: Structure and NMMO processability of the pulps.
440 *Cellulose*, *11*(1), 85–98. https://doi.org/10.1023/B:CELL.0000014779.93590.a0

441 Fink, H. P., Weigel, P., Purz, H. J., & Ganster, J. (2001). Structure formation of regenerated
442 cellulose materials from NMMO-solutions. *Progress in Polymer Science*, *26*(9), 1473–1524.
443 https://doi.org///dx.doi.org/10.1016/S0079-6700(01)00025-9

444 Gübitz, G. M., Stebbing, D. W., Johansson, C. I., & Saddler, J. N. (1998). Lignin-hemicullulose
445 complexes restrict enzymatic solubilization of mannan and xylan from dissolving pulp.
446 *Applied Microbiology and Biotechnology*, *50*(3), 390–395.
447 https://doi.org/10.1007/s002530051310

448 Hailwood, A. J., & Horrobin, S. (1946). Absorption of water by polymers: analysis in terms of a
449 simple model. *Transactions of the Faraday Society*, *42*(0), B092.
450 https://doi.org/10.1039/TF946420B084

451 Hauru, L. K. J., Ma, Y., Hummel, M., Alekhina, M., King, A. W. T., Kilpelainen, I., … Sixta, H.
452 (2013). Enhancement of ionic liquid-aided fractionation of birchwood. Part 1: autohydrolysis
453 pretreatment. *RSC Advances*, *3*(37), 16365–16373. https://doi.org/10.1039/C3RA41529E

454 Hermanutz, F., Meister, F., & Uerdingen, E. (2006). New developmens in the manufacture of
455 cellulose fibres with ionic liquids. *Chemical Fibers International*, *56*, 342–343.

456 Hummel, M., Michud, A., Tanttu, M., Asaadi, S., Ma, Y., Hauru, L. K. J., … Sixta, H. (2015).
457 Ionic liquids for the production of man-made cellulosic fibers: Opportunities and challenges.
458 *Advances in Polymer Science*, *217*, 133-168. https://doi.org/10.1007/12_2015_307

459 Hämmerle, F. M. (2011). The cellulose gap (the future of cellulose fibres). *Lenzinger Berichte*, *89*,

12–21.

Imamura, R., Murakami, K., & Ueno, T. (1972). Depolymerization of cellulose by electron beam irradiation. *Bulletin of the Institute for Chemical Research, Kyoto University*, *50*(1), 51–63.

Jiang, W., Sun, L., Hao, A., & Chen, J. Y. (2011). Regenerated Cellulose Fibers From Waste Bagasse Using Ionic Liquid. *Textile Research Journal*, *81*, 1949–1958.

Kassim, M. A., Khalil, H. P. S. A., Serri, N. A., Kassim, M. H. M., Syakir, M. I., Aprila, N. A. S., & Dungani, R. (2016). Irradiation Pretreatment of Tropical Biomass and Biofiber for Biofuel Production. In *Radiation Effects in Materials* (pp. 329–356). Rijeka: InTech. https://doi.org/10.5772/62728

Khan, A. W., Labrie, J. P., & McKeown, J. (1986). Effect of electron-beam irradiation pretreatment on the enzymatic hydrolysis of softwood. *Biotechnology and Bioengineering*, *28*(9), 1449–1453. https://doi.org/10.1002/bit.260280921

Kong, K., & Eichhorn, S. J. (2005). Crystalline and amorphous deformation of process-controlled cellulose-II fibres. *Polymer*, *46*(17), 6380–6390. https://doi.org///dx.doi.org/10.1016/j.polymer.2005.04.096

Kreze, T., & Malej, S. (2003). Structural Characteristics of New and Conventional Regenerated Cellulosic Fibers. *Textile Research Journal*, *73*(8), 675–684.

Kristiani, A., Effendi, N., Styarini, D., Aulia, F., & Sudiyani, Y. (2016). The Effect of Pretreatment by using Electron Beam Irradiation On Oil Palm Empty Fruit Bunch. *Atom Indonesia*, *42*(1), 9. https://doi.org/10.17146/aij.2016.472

Le, H. Q., Ma, Y., Borrega, M., & Sixta, H. (2016). Wood biorefinery based on gamma]-

valerolactone/water fractionation. *Green Chemistry*, *18*(20), 5466–5476. https://doi.org/10.1039/C6GC01692H

Lee, B.-M., Lee, J.-Y., Kim, D.-Y., Hong, S.-K., Kang, P.-H., & Jeun, J.-P. (2014). Environmentally-Friendly Pretreatment of Rice Straw by an Electron Beam Irradiation. *Korean Society for Biotechnology and Bioengineering Journal*, *29*(4), 297–302. https://doi.org/10.7841/ksbbj.2014.29.4.297

Leppänen, K., Bjurhager, I., Peura, M., Kallonen, A., Suuronen, J.-P., Penttilä, P., … Serimaa, R. (2011). X-ray scattering and microtomography study on the structural changes of never-dried silver birch, European aspen and hybrid aspen during drying. *Holzforschung*, *65*(6), 865–873. https://doi.org/10.1515/HF.2011.108

Ma, Y., Asaadi, S., Johansson, L.-S., Ahvenainen, P., Reza, M., Alekhina, M., … Sixta, H. (2015a). High-Strength Composite Fibers from Cellulose–Lignin Blends Regenerated from Ionic Liquid Solution. *ChemSusChem*, *8*(23), 4030–4039. https://doi.org/10.1002/cssc.201501094

Ma, Y., Asaadi, S., Johansson, L. S., Ahvenainen, P., Reza, M., Alekhina, M., … Sixta, H. (2015b). High-Strength Composite Fibers from Cellulose-Lignin Blends Regenerated from Ionic Liquid Solution. *ChemSusChem*, *8*(23), 4030–4039. https://doi.org/10.1002/cssc.201501094

Ma, Y., Hummel, M., Maattanen, M., Sarkilahti, A., Harlin, A., & Sixta, H. (2016). Upcycling of waste paper and cardboard to textiles. *Green Chemistry*, *18*(3), 858–866. https://doi.org/10.1039/C5GC01679G

Maurer, R. J., Sax, A. F., & Ribitsch, V. (2013). Moleular simulation of surface reorganization and wetting in crystalline cellulose I and II. *Cellulose*, *20*(1), 25–42.

https://doi.org/10.1007/s10570-012-9835-9

Michud, A., Hummel, M., & Sixta, H. (2015). Influence of molar mass distribution on the final properties of fibers regenerated from cellulose dissolved in ionic liquid by dry-jet wet spinning. *Polymer*, *75*, 1–9. https://doi.org///dx.doi.org/10.1016/j.polymer.2015.08.017

Michud, A., Hummel, M., & Sixta, H. (2016). Influence of process parameters on the structure formation of man-made cellulosic fibers from ionic liquid solution. *Journal of Applied Polymer Science*, *133*(30), n/a. https://doi.org/10.1002/app.43718

Michud, A., King, A., Parviainen, A., Sixta, H., Hauru, L., Hummel, M., & Kilpeläinen, I. (2014). Process for the production of shaped cellulose articles.

Michud, A., Tanttu, M., Asaadi, S., Ma, Y., Netti, E., Kääriainen, P., … Sixta, H. (2016). Ioncell-F: ionic liquid-based cellulosic textile fibers as an alternative to viscose and Lyocell. *Textile Research Journal*, *86*(5), 543–552. https://doi.org/10.1177/0040517515591774

Mosier, N., Wyman, C., Dale, B., Elander, R., Lee, Y. Y., Holtzapple, M., & Ladisch, M. (2005). Features of promising technologies for pretreatment of lignocellulosic biomass. *Bioresource Technology*, *96*(6), 673–686. https://doi.org/10.1016/j.biortech.2004.06.025

Okubayashi, S., Griesser, U. J., & Bechtold, T. (2004). A kinetic study of moisture sorption and desorption on lyocell fibers. *Carbohydrate Polymers*, *58*(3), 293–299. https://doi.org///dx.doi.org/10.1016/j.carbpol.2004.07.004

Okubayashi, S., Griesser, U. J., & Bechtold, T. (2005a). Moisture sorption/desorption behavior of various manmade cellulosic fibers. *Journal of Applied Polymer Science*, *97*(4), 1621–1625. https://doi.org/10.1002/app.21871

523 Okubayashi, S., Griesser, U. J., & Bechtold, T. (2005b). Water Accessibilities of Man-made
524 Cellulosic Fibers – Effects of Fiber Characteristics. *Cellulose*, *12*(4), 403–410.
525 https://doi.org/10.1007/s10570-005-2179-y

526 Parviainen, A., King, A. W. T., Mutikainen, I., Hummel, M., Selg, C., Hauru, L. K. J., …
527 Kilpeläinen, I. (2013). Predicting Cellulose Solvating Capabilities of Acid-Base Conjugate
528 Ionic Liquids. *ChemSusChem*, *6*(11), 2161–2169. https://doi.org/10.1002/cssc.201300143

529 Rosenau, T., Potthast, A., Sixta, H., & Kosma, P. (2001). The chemistry of side reactions and
530 byproduct formation in the system NMMO/cellulose (Lyocell process). *Progress in Polymer*
531 *Science (Oxford)*, *26*(9), 1763–1837. https://doi.org/10.1016/S0079-6700(01)00023-5

532 Siroka, B., Noisternig, M., Griesser, U. J., & Bechtold, T. (2008). Characterization of cellulosic
533 fibers and fabrics by sorption/desorption. *Carbohydrate Research*, *343*(12), 2194–2199.
534 https://doi.org///dx.doi.org/10.1016/j.carres.2008.01.037

535 Sixta, H. (2006). Chemical Pulping Processe: Sections 4.2.8–4.3.6.5. In *Handbook of Pulp* (pp.
536 366–509). Weinheim, Germany: Wiley-VCH Verlag GmbH.
537 https://doi.org/10.1002/9783527619887.ch4c

538 Sixta, H., Michud, A., Hauru, L., Asaadi, S., Ma, Y., King, A. W. T., … Hummel, M. (2015).
539 Ioncell-F: A High-strength regenerated cellulose fibre. *Nordic Pulp and Paper Research*
540 *Journal*, *30*(1), 043–057. https://doi.org/10.3183/NPPRJ-2015-30-01-p043-057

541 Skaar, C. (1988). Theories of Water Sorption by Wood. In *Wood-Water Relations* (pp. 86–121).
542 Berlin: Springer Berlin Heidelberg. https://doi.org/10.1007/978-3-642-73683-4_3

543 Stana-Kleinschek, K., Ribitsch, V., Kreže, T., Sfiligoj-Smole, M., & Peršin, Z. (2003). Correlation

544 of regenerated cellulose fibres morphology and surface free energy components. *Lenzinger*
545 *Berichte*, *82*, 83–95.

546 Sun, N., Li, W., Stoner, B., Jiang, X., Lu, X., & Rogers, R. D. (2011). Composite fibers spun
547 directly from solutions of raw lignocellulosic biomass dissolved in ionic liquids. *Green*
548 *Chemistry*, *13*(5), 1158–1161. https://doi.org/10.1039/C1GC15033B

549 Sun, N., Rahman, M., Qin, Y., Maxim, M. L., Rodriguez, H., & Rogers, R. D. (2009). Complete
550 dissolution and partial delignification of wood in the ionic liquid 1-ethyl-3-
551 methylimidazolium acetate. *Green Chemistry*, *11*(5), 646–655.
552 http://dx.doi.org/10.1039/B822702K

553

554
555

556

557